Mechanism of Anion-Catalyzed C–H Silylation Using TMSCF3: Kinetically-Controlled CF3-Anionoid Partitioning As a Key Parameter

Mechanism of Anion-Catalyzed C-H Silylation using $TMSCF_3$: Kinetically-Controlled CF_3-anionoid Partitioning as a Key Parameter

Andrés García-Domínguez, Pedro H. Helou de Oliveira, Gilian T. Thomas,[†]
Arnau R. Sugranyes[§] and Guy C. Lloyd-Jones*

EaStChem, University of Edinburgh, Joseph Black Building, David Brewster Road, Edinburgh, EH9 3FJ, UK.

Keywords: Kinetics, Stopped-Flow NMR, Silanes, Partitioning, Carbenes, Deprotonation, Kinetic Acidity, Weak C-H acids

ABSTRACT: The mechanism of anion-catalyzed C-H silylation by R_3SiCF_3 reagents has been investigated using homogeneous TBAT-initiation, in situ and stopped-flow ^{19}F-NMR spectroscopy, ^{2}H-KIE, LFER, deuterium-labelled cross-over, structure-selectivity quantitation ($TMSCF_3$ / $TESCF_3$), carbene trapping, and DFT-calculations. Analysis of the kinetics of reactions of 1,3-difluorobenzenes (**2**), and the generation of $ArSiMe_3$ and Me_3SiF as a function of the concentration of [**2**], [$TMSCF_3$] and [TBAT], show that a CF_3-anionoid is the active intermediate. The CF_3-anionoid is reversibly released from siliconate $[(CF_3)_2SiMe_3]^-$, and undergoes partitioning through rate-limiting arene deprotonation (^{1}H/^{2}H KIE 9.5) to generate $ArSiMe_3$ (via a transient aryl anionoid) and fluoroform (CF_3H), in competition with F-anion transfer to $TMSCF_3$ to generate CF_2 and TMSF. The [**2**]/[$TMSCF_3$] concentration ratio directly and proportionally controls the kinetics of the partition, in favor of C-H deprotonation. Higher concentrations of TBAT and lower concentrations of $TMSCF_3$ lead to faster rates of $ArSiMe_3$ generation. Use of the homologous $TESCF_3$ reagent leads to faster rates of anion catalysis, and an increased selectivity towards C-H deprotonation. Perfluoroalkenes, generated in situ from CF_2, capture the CF_3-anionoid leading to progressive inhibition of the anion-catalysis. Inhibition is suppressed by using a styrene additive to trap the CF_2, and the efficiency of the process enhanced by slow-addition of $TMSCF_3$ (**1**) to maintain a high concentration ratio [**2**] / [**1**].

INTRODUCTION

Over the last decade there has been surge of interest in the use of trifluoromethyltrimethylsilane (**1**, $TMSCF_3$) as a reagent for the preparation of fluorine-containing molecules.[1] The reagent is commercially-available, at scale, relatively inexpensive, has low toxicity, a long shelf-life, is easily handled (b.p. = 55 °C), and has a very wide scope of applications (Scheme 1A);[1-6] all features that have contributed to its popularity. Beginning with the pioneering work of Ruppert,[4] and Prakash,[5] three general classes of anion-catalyzed[2] reactions of $TMSCF_3$ have been developed: the transfer of CF_3 to electrophiles, (e.g. ketones, i),[6] the generation and trapping of CF_2, (e.g. in alkene cycloaddition, ii);[7] and C-H functionalization,[8-13] typically RH → RTMS, iii), for example in the silylation[14,15] of suitably reactive arenes.[10,13] All three of these processes require silaphilic initiation (X^-), most-commonly a fluoride source.

We recently reported on the mechanisms involved in reactions (i)[16] and (ii),[17] Scheme 1B. Addition of a catalytic quantity of $[Ph_3SiF_2][Bu_4N]$ ('TBAT')[18] to $TMSCF_3$ at ambient temperature results in the rapid generation of an equilibrium mixture (K_1) of $[(CF_3)_2SiMe_3]^-$, $TMSCF_3$ (**1**) and a CF_3-anionoid, Scheme 1C. It is this fluxional, highly-reactive, and metastable mixture[16,17,19] that serves as a source of both CF_3 and CF_2, depending on the reaction conditions.[16-20] For both reactions (i and ii), use of anhydrous conditions and aprotic solvents is essential to avoid competing, or exclusive, conversion of **1** to fluoroform (CF_3H).[17,21a,c]

Scheme 1. (A) Generic reactivity of $TMSCF_3$ (1). (B) Anion-catalyzed Reactions of 1 with carbonyls (i),[6,16] alkenes (ii),[7,17] and weak C-H acids (RH) (iii).[10,13] (C) Equilibrium (K_1) Between $[(CF_3)_2SiMe_3]^-$, $TMSCF_3$ (1) and $[CF_3]^-$.[16,17,19]

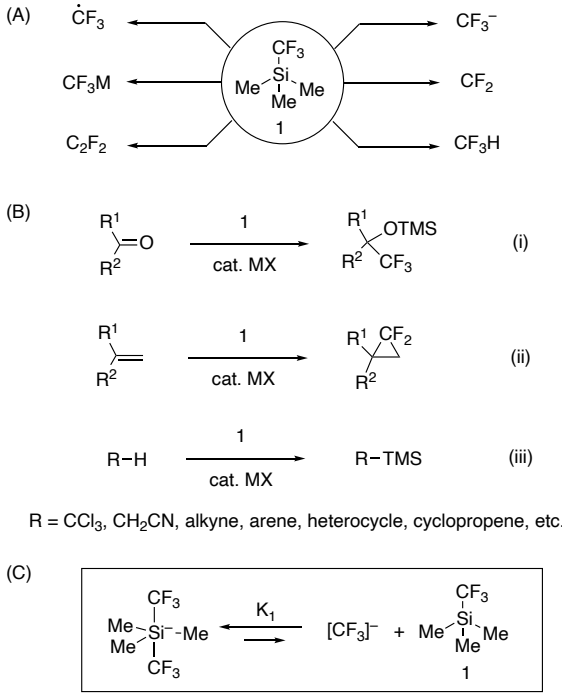

However, this latter mode of CF_3H production from $TMSCF_3$ (**1**) can be valuably harnessed to generate and trap transient organic anions from weakly C-H acidic species, Scheme Biii, including MeCN,[8,9] CH_2Cl_2,[9] $CHCl_3$,[10] indenes,[10] cyclopropenes,[11b] activated alkyl sulphones,[10] terminal alkynes,[12] and more recently arenes.[10,13] Indeed, the scope of the latter reaction has been substantially expanded by Kondo, to allow highly regioselective C-H silylation of nitrobenzenes, (benzo)thiophenes, benzofurans, and fluorobenzenes.[13] Although fluoroform (CF_3H) has been qualitatively identified as a co-product in some examples of C-H silylation by **1** (Scheme Biii),[9,11b,13a] the roles of siliconates and the reagent ($TMSCF_3$, **1**) have not been elucidated. Nor have the factors that govern the overall feasibility of the reaction class in general, or the apparent requirement for excess $TMSCF_3$ (**1**), typically 2-3 equivalents, and high loading (20-50 mol%) of anionic initiator. Herein we report on the kinetics and mechanism of C-H silylation (Scheme Biii). To do this, we have used the reactions of 1,3-difluorobenzenes (**2**) described by Kondo,[13] as a versatile platform for analysis by ^{19}F and ^{29}Si NMR spectroscopy, LFER, KIEs, and DFT.

RESULTS AND DISCUSSION

Preliminary Studies We began by analysis of the silylation of **2a** (X=H) using $TMSCF_3$ (**1**, 2.1 equiv) under the heterogeneous reaction conditions reported by Kondo (1.0 M **2a**, 50 mol% CsF, 273 K, DME, 2 h).[13a] ^{19}F NMR spectroscopy of the product mixture indicated partial conversion of **2a** to **3a** (61%). Replacing CsF with 5 mol % TBAT[18] as a soluble anionic initiator in anhydrous THF at 300 K, gave similar results (68% conversion of **2a** to **3a**). The homogeneous reaction conditions allowed monitoring of the process by in situ ^{19}F NMR spectroscopy, as well as direct use of kinetic constants previously established for equilibrium K_1 (Scheme 1C).[16,17] However, to avoid dangerous overpressures[21] caused by outgassing of rapidly-evolved CF_3H (b.p. –82 °C), we used lower concentrations of **1** and **2a**, Figure 1.

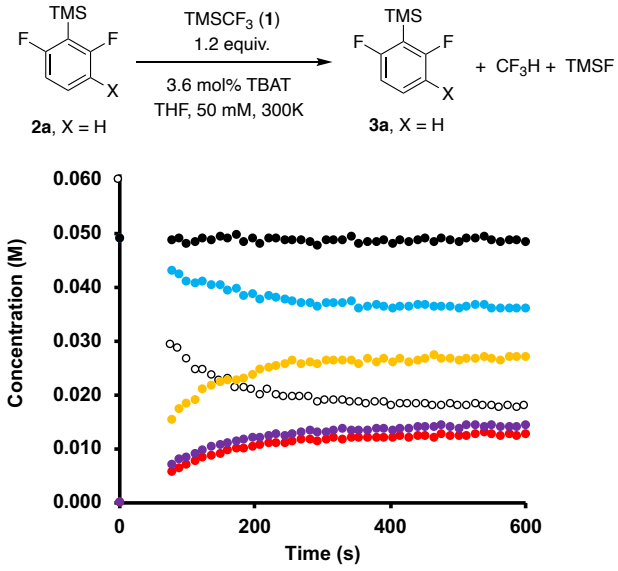

Figure 1. Preliminary in situ ^{19}F NMR spectroscopic analysis of the anion-catalyzed reaction of $TMSCF_3$ with **2a**. Conditions: $[\mathbf{1}]_0$ 60 mM, $[\mathbf{2a}]_0$ 50 mM, TBAT 1.8 mM, 300K, THF. Manual assembly and then analysis by ^{19}F NMR spectroscopy at 300 K; for full details, see SI, section 2.3

The reactions were found to proceed relatively rapidly, resulting in absence of data for the first ~80 seconds after manual assembly of the reaction in the NMR tube. Nonetheless, the in situ ^{19}F NMR spectroscopic analysis confirmed dynamic line broadening of $TMSCF_3$ (**1**), indicative of the expected rapid equilibrium involving $[(CF_3)_2SiMe_3]^-$ (Scheme 1C) and after an initial burst of CF_3H, corresponding to consumption of trace water (22-25 ppm, KF titration), the evolution of $[CF_3H]$ and [Ar-TMS] (**3a**) were directly proportional. The reactions stalled after approximately 400 seconds, at which point ~70% of **1** had been consumed, Figure 1. Further experiments employing [2D]-**2a** (see SI, section 3) confirmed that the dueteron of the C-D acid ([2D]-**2a)** emerges in CF_3D.[9,11] Moreover, there was no detectable de-silylation of the product (**3a**) evident from studies of the co-reaction of **2a** and 4-D-**3a**. However, in cases where there was complete consumption of **1**, there is a slow degenerate trimethylsilyl exchange between **2a** and **3a** (see SI, Section 3).

Reaction Kinetics, KIE and LFER Using variable-ratio stopped-flow ^{19}F NMR spectroscopy,[16] where NMR spectra can be acquired within 0.2 seconds of initiation of the reaction, a wide range of initial concentrations[22] of $TMSCF_3$ (**1**), arene (**2a**), and TBAT, were explored, Figure 2. Together with kinetic simulations (SI section 8.6), the data show that productive turnover of **2a** to **3a** has a first order dependence on both the arene ($[\mathbf{2a}]_t$) and the active anion concentration, ($x[\text{TBAT}]_0$; $1 \geq x \geq 0$), with $TMSCF_3$ (**1**) acting as an inhibitor to the process. The latter results in the reactions exhibiting a marked acceleration in the rate of generation of **3a** when the evolving ratio $[\mathbf{2a}]_t/[\mathbf{1}]_t$ rises above unity. The latter evident for example in Figure 2B, $[\mathbf{2a}]_0$.= 51 mM, where the reaction profile switches from progressive deceleration to progressive acceleration, when $[\mathbf{1a}]_0$ is reduced from 53 mM to 66 mM.

The inhibitory effect of [**1**] on the rate of generation of **3a**, indicates that the active intermediate is a CF_3-anionoid, not the siliconate $[(CF_3)_2SiMe_3]^-$ from which it is reversibly released ($1/K_1$). Irreversible rate-limiting deprotonation of the C-H acid by the CF_3-anionoid will generate CF_3H plus a transient anionoid, which on rapid silylation by $TMSCF_3$ (**1**), releases aryl-TMS (**3a**) and regenerates the CF_3-anionoid. Evidence to support this conclusion comes from a large primary kinetic isotope effect at the arene C-H ($k_H/k_D = 9.5$ for the reaction of **2a** versus 2-D-**2a**, see SI, Section 5). DFT calculations for proton transfer, after pre-complexation of the CF_3-anion and application of a tunneling correction, afforded a KIE value consistent with this process ($k_H/k_D = 9.7$; see SI, Section 11.3). Furthermore, a linear free energy relationship (LFER) constructed by intermolecular competition of a series of 4-substituted-1,3-difluorobenzenes gave a large positive correlation ($\rho = +5.5$) indicative of a substantial accumulation of negative charge[23] at the transition state (Figure 2D). A computationally-assessed LFER was in good agreement ($\rho_{calc} = 1.2\ \rho_{exp}$; see SI, Section 11.2).

Whilst the preliminary analysis indicates some similarity to CF_3-transfer from **1**,[16] there are some important differences in the factors affecting selectivity and efficiency. Thus, in stark contrast to the highly efficient trifluoromethylation of ketones (Bi),[4-6] multiple side-products are generated in the aryl silylation reaction (Biii). These do not arise from **2a** or **3a** (see material balance, Figure 1) but instead from the $TMSCF_3$ (**1**). Moreover, the reactions show clear signs of progressive inhibition of the anionic catalysis, see e.g. Figure 2C where $[\text{TBAT}]_0 \leq 2.1$ mM, in some cases resulting in complete stalling ($x \rightarrow 0$) of the process prior to completion, Figure 1.

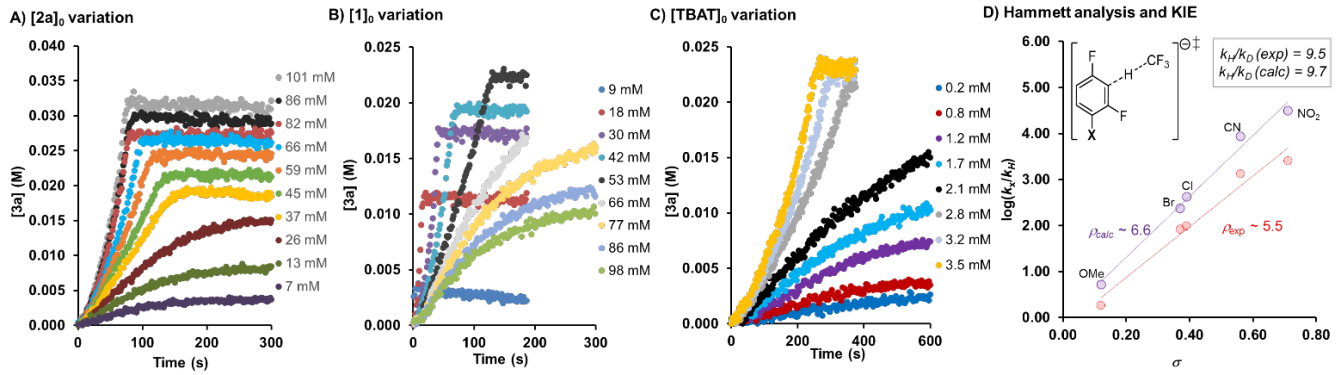

Figure 2. Kinetics, LFER and KIE for the Anion-Catalyzed Reaction of $TMSCF_3$ (1) with 2. Conditions: (**A**) [**1**]$_0$ 63 mM, TBAT 3.6 mM, 300 K, with [**2**]$_0$ varied from 7 to 101 mM; (**B**) [**2a**]$_0$ 51 mM, TBAT 3.6 mM, 300 K, with [**1**]$_0$ varied from 9 to 98 mM; (**C**) [**1**]$_0$ 65 mM, [**2a**]$_0$ 53 mM, 293K, with [TBAT]$_0$ varied from 0.2 to 3.5 mM (0.37 to 6.6 mol%; (**D**) Experimental and computed KIE and linear free energy relationship for C-H deprotonation by CF3 anionoid, see SI, sections 5, 6, 11.2, and 11.3 for full details.

Productive Fractionation and Progressive Inhibition ^{19}F NMR spectroscopic analysis of the evolution of the side-products in the reaction system revealed two key features. Firstly, correlation of the growth of [**3a**]$_t$ against [TMSF]$_t$ affords the productive fractionation of reagent **1** into C-H silylation product **3a** versus TMSF (*f*, equation 1).

$$f = \frac{\nu_{3a}}{\nu_{TMSF}} \quad \text{eq. 1}$$

Analysis of the *initial* productive fractionation, f_0, across a wide range of initial concentrations of $TMSCF_3$ [**1**]$_0$, arene [**2a**]$_0$, and anion [TBAT]$_0$, confirmed a simple dependency on the concentration ratio of the reactants, where $f_0 \approx (0.44\ [\mathbf{2a}]_0 / [\mathbf{1}]_0)$, see Figure 3A This relationship is independent of the anion concentration, [TBAT]$_0$, Figure 3B. However, due to the side reactions that consume **1**, the reactant ratio ([**2a**]$_t$/[**1**]$_t$) increases as the reaction evolves and the productive fractionation, *f*, rises until **2a** is fully depleted (see SI section 4.4).

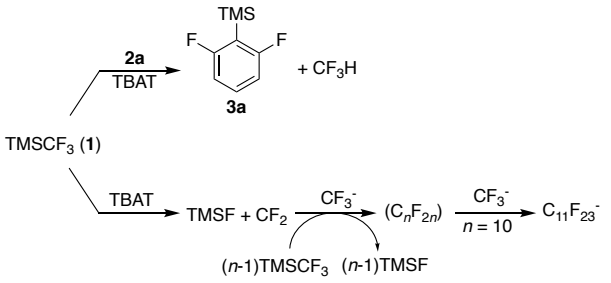

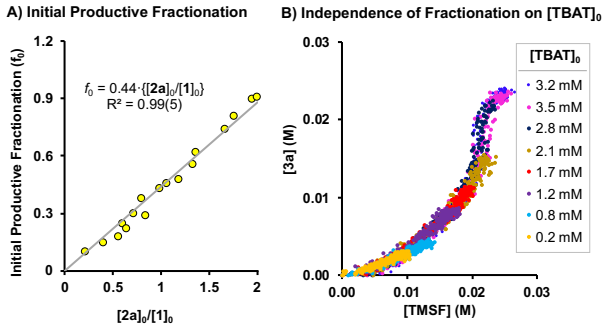

Figure 3. A) Initial productive fractionation, f_0 equation 1. B) Evolution of silylation product 3a versus TMSF at various [TBAT]$_0$. See SI section 4.4 for full details.

Secondly, the reactions progressively generated $[C_{11}F_{23}]^-$ (**4**),[17,24] a species that we have previously identified as the product of sequential additions of the CF_3-anionoid to in situ generated perfluoroalkenes. Fluoride elimination from perfluorocarbanion **4** is strongly disfavored because both of the isomers of the corresponding perfluoroalkene are highly strained.[17] As a consequence, progressive generation of $[C_{11}F_{23}]^-$ (**4**) results in eventual termination of the anionic catalysis in reaction (iii).

$TESCF_3$ versus $TMSCF_3$ The use of alternative reagents to **1**, such as commercially-available $TESCF_3$ (**7**), has been reported, in a few examples, to give analogous silylated products to reaction (iii),[13] but with no detail on the rate or selectivity. Based on our previous studies of reactions (i) and (ii), the increased steric bulk and changes in electron density at silicon in the TES moiety are expected to have a considerable impact on the kinetics and partitioning.[16,17] Reaction of **2a** with $TESCF_3$ (**7**) confirmed the same general features as found with reactions using $TMSCF_3$, i.e. co-evolution of CF_3H with the Ar-TES product (**8a**), and continuous TESF generation. However, compared to **1**, the equilibrium of **7** with siliconate $[(CF_3)_2SiEt_3]^-$ is less favoured (calc. $K_1^{TMS} / K_1^{TES} \approx 20$)[17] leading to higher equilibrium concentrations of the CF_3-anionoid.[16] Stopped-flow ^{19}F NMR spectroscopy of the reaction confirmed considerably faster anion-catalyzed reaction of **2a** with $TESCF_3$ (**7**), as compared to $TMSCF_3$ (**1**). Indeed, reactions conduced *solely* with $TESCF_3$ (**7**) required reduced catalyst loading (1.8 mol% TBAT) and higher substrate concentrations to allow ^{19}F NMR spectroscopic monitoring of the reaction evolution, which still proceeded to 95% conversion in about 7 seconds, Figure 4A. Moreover, when normalized by reactant ratio ([**2a**]$_0$/[**1**,**7**]$_0$), reactions with $TESCF_3$ (**7**) proceed with about twenty-fold greater initial productive fractionation, f_0, than **1**, consistent with the lower propensity for TESF + $(CF_2)_n$ generation from **7**.[17]

To further compare the reactivity of the two silanes we co-reacted them with arene **2a** under various conditions, see Figure 4B (and SI Section 7 for further examples), revealing some remarkable features. Consistent with **7** being the more hindered silylating reagent, transfer of the TMS group to generate **3a**, occurs preferentially to transfer of TES, to generate **8a**. However, the process by which this occurs is not simply a direct competition between reagents **1** and **7**. For example, after initiation of anionic catalysis, an equimolar mixture of **1** and **7** generate the

corresponding fluorosilanes, TMSF and TESF, at a similar initial rate: v_0TMSF/v_0TESF ~1, but the silylation product is almost exclusively Ar-TMS (**3a**). We have previously shown that the isodesmic equilibrium shown in Scheme 2 (K_{Si}, $\Delta G_{300} \leq 0.2$ kcal/mol, DFT) is catalyzed by the CF_3-anionoid,[17] and during reaction of **2a** with **1** + **7**, there is dynamic line-broadening of both the TESF and TMSF signals in the ^{19}F NMR spectrum, see SI Section 7.2B. A large proportion of the $TMSCF_3$ (**1**) also undergoes competing decomposition to TMSF. However, the TMSF is recycled to $TMSCF_3$ by the $TESCF_3$ with co-generation of TESF, Scheme 2. Consequently, for first part of the reaction (Fig 4B), the nascent aryl anion from **2a**, predominantly reacts with $TMSCF_3$ (**1**) leading to generation of **3a**. As the system evolves, the available sources of TMS (**1** + TMSF) are progressively depleted and the nascent aryl anion from **2a** is increasingly captured by $TESCF_3$ (**7**) to generate **8a**, with very little competing generation of TESF. Notably, the $TMSCF_3$ is a more powerful inhibitor than $TESCF_3$ (**7**), and the rate is supressed compared to using solely $TESCF_3$ (**7**); compare Figures 4A and 4B.

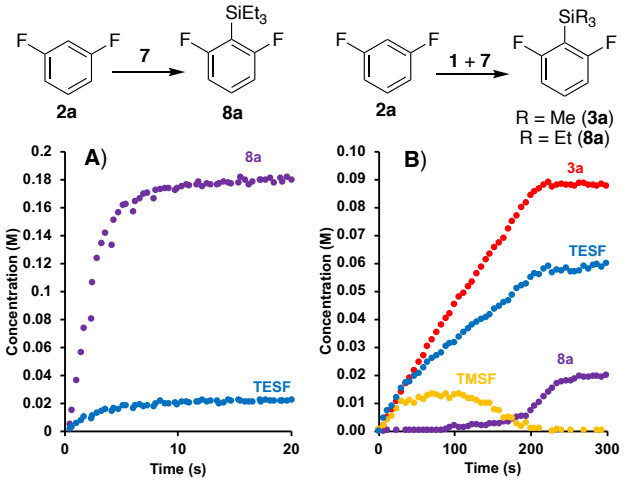

Figure 4. (A) Reactivity of $TESCF_3$ as silylating agent; (B) Co-reaction of $TESCF_3$ with $TMSCF_3$. Conditions: (A), $[7]_0$ 220 mM, $[2a]_0$ 200 mM, TBAT 1.8 mo% (3.6 mM), 300K, THF. (B) $[1]_0 = [7]_0$ 105 mM, $[2a]_0$ 175 mM, TBAT 3.1 mol% (5.4 mM) 300K. The much faster reactions with solely **7** (Figure A) required lower catalyst loadings and higher substrate concentrations for effective analysis by variable-ratio stopped-flow ^{19}F NMR spectroscopy at 300 K, for full details, see SI, section 7.

Scheme 2. $TMSCF_3$ regeneration in situ from $TESCF_3$.

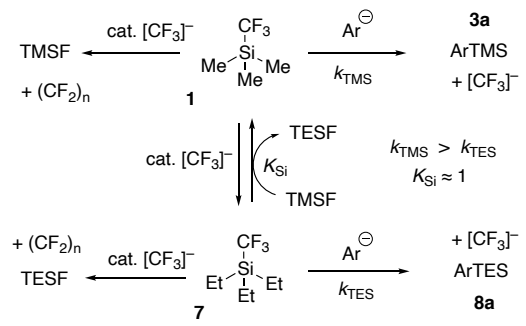

Overarching Mechanism for Anion-catalyzed Silylation of Weak C-H acids by $TMSCF_3$ The investigation outlined above allows the construction of a general mechanism for the C-H silylation process, Scheme 3. The key steps are: i) rapid release of a CF_3-anionoid (k_{-1}, 4 $\times 10^3$ s^{-1}, at 300 K)[17] from the dominant anion, siliconate $[(CF_3)_2SiMe_3]^-$; ii) reaction of the CF_3-anionoid with the C-H acid (RH, k_2) to generate CF_3H. iii) silylation of the resultant transient carbanion ($[R]^-$, k_4) by $TMSCF_3$; iv) complexation of the CF_3-anionoid with $TMSCF_3$ (k_1) to regenerate $[(CF_3)_2SiMe_3]^-$; v) fluoride-transfer (k_3) from the CF_3-anionoid to $TMSCF_3$ to generate CF_2 and fluorosiliconate $[(CF_3)Si(F)Me_3]^-$;[19] vi) TMSF dissociation (k_{-5}); and vii) anion-mediated homologation (k_6) generating perfluoroalkenes (C_nF_{2n}). The two competing processes (k_2 and k_3) kinetically-control and thus govern the feasibility of the process: the greater the kinetic C-H acidity of the substrate (RH, k_2), the greater the intrinsic efficiency. For arene **2a**, the CF_3-anionoid partitioning (Figure 3) makes the process feasible but rather inefficient, with a significant proportion of the $TMSCF_3$ (**1**) being consumed non-productively via k_3, and subsequent CF_3-anionoid catalyzed homologation (n) by **1**, co-generating further TMSF.

Scheme 3. General Mechanism for Anion-Catalyzed Silylation of weak C-H acids (R-H) by $TMSCF_3$ (1).

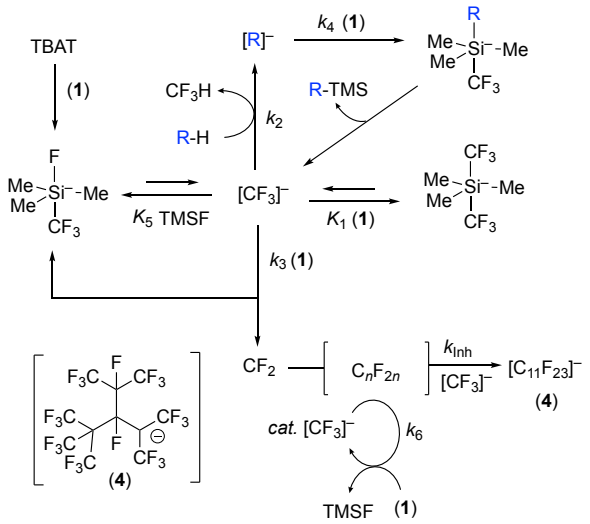

Practical implications of the CF_3-anion partition (k_2/k_3) For the general mechanism shown in Scheme 3, the rate of consumption of $TMSCF_3$ (**1**) is described by equation 2, where x is the mol-fraction of anion in non-terminated form ($1 \geq x \geq 0$) and n is the average degree of anion-induced homologation (k_6). The productive fractionation, f, of $TMSCF_3$ (**1**) into the silylation product (RTMS) is given by equation 3, and the rate of generation of the silylation product by equation 4. Although the partitioning constants (k_2, k_3) are fixed (k_2 by the kinetic acidity of the C-H acid, and k_3 by the reagent **1**), equations 2-4 guide the design of reaction conditions to maximize the rate and efficiency of the process.

$$\frac{-d[\mathbf{1}]}{dt} \approx \frac{x[\mathrm{TBAT}]_0\,(k_2[\mathrm{RH}]_t + n.k_3[\mathbf{1}]_t)}{1 + K_1[\mathbf{1}]_t + K_5[\mathrm{TMSF}]_t} \qquad \text{eq. 2}$$

$$f_t = \frac{v_{\mathrm{RTMS}}}{v_{\mathrm{TMSF}}} \approx \frac{k_2[\mathrm{RH}]_t}{n.k_3[\mathbf{1}]_t} \qquad \text{eq. 3}$$

$$\frac{d[\mathrm{RTMS}]}{dt} \approx \frac{x[\mathrm{TBAT}]_0\,k_2[\mathrm{RH}]_t}{1 + K_1[\mathbf{1}]_t + K_5[\mathrm{TMSF}]_t} \qquad \text{eq. 4}$$

For example, the greater the extent of anion-induced homologation, (k_6; $n \geq 1$) the more extensive the progressive inhibition (k_{Inh}) of catalysis. Thus, for a given initial concentration of C-H acid (RH) and **1**, there will be a minimum initial anion concentration ([TBAT]$_0$) required to reach full conversion of **1**; below this value reactions stall due to complete anion sequestration in species such as $[C_{11}F_{23}]^-$ (**4**). For example, stopped-flow ^{19}F NMR spectroscopic analysis of the reaction of [**2a**]$_0$ = 150 mM, with [**1**]$_0$ = 180 mM, initiated by 5.3 mol% TBAT, shows progressive inhibition approximately 30 seconds after initiation, and the reaction eventually stalls ($x \rightarrow 0$) reaching ~30% conversion of **2a** to **3a**, Figure 5.

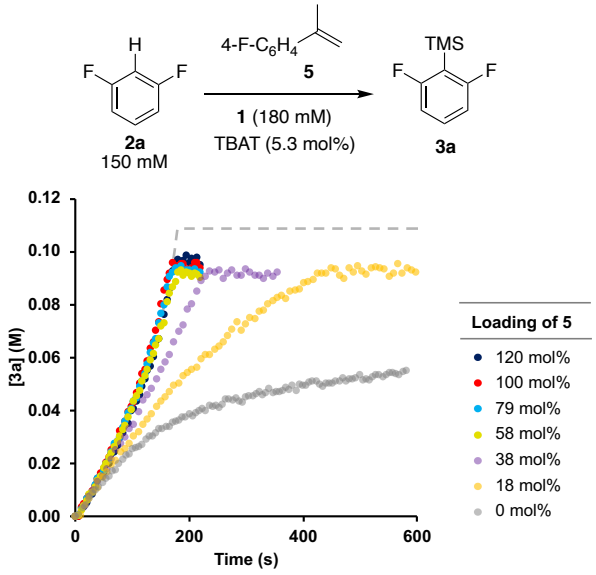

Figure 5. Use of an alkene additive (**5**) to trap CF_2, and sustain anionic catalysis of the C-H silylation process (**2a** → **3a**). Analysis by variable-ratio stopped-flow ^{19}F NMR spectroscopy at 300 K, for full details, see SI section 8.4. Dashed line is the calculated limiting rate and efficiency (equations 3 and 4, n = 1) see SI section 8.6.

Scheme 4. Maximizing productive fractionation, *f*, equation 3, by maintaining a high concentration ratio of [2a]/[1].[a]

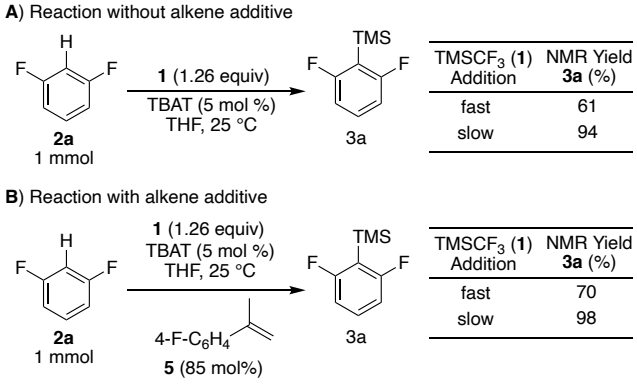

TMSCF$_3$ (**1**) Addition	NMR Yield **3a** (%)
fast	61
slow	94

TMSCF$_3$ (**1**) Addition	NMR Yield **3a** (%)
fast	70
slow	98

[a] Conditions: **1** added as a 2.1 M solution in under 2 sec ('fast') or over 72 mins ('slow') to a solution of **2a** (2.5 M) + TBAT. [**2a**+**3a**]$_{final}$ = 1.0 M; [Si]$_{final}$ = 1.26 M. For full details, see SI, section 8.2.

One way to attenuate the anion-induced homologation (k_X) is by diverting the nascent difluorocarbene.[7,17] This has the effect of increasing the productive fractionation, in the limit to n = 1 (equation 3), and in doing so attenuating the progressive inhibition *via* perfluoroalkene generation. By using styrene **5** (18 mol%; Figure 5) as an efficient CF_2 trap, the reaction proceeds to completion (100 % conversion of **1**) and with ~60% conversion of **2a** to **3a**. Increased co-loadings of styrene **5** lead to faster overall rates of generation of **3a**, up to a limiting value beyond which the active anion is maintained throughout ($x \approx 1$). Kinetic simulations (see SI section 8.6) suggest that k_2/k_3 = 1.1, and thus in the absence of alkene additive (Figure 3) $n \approx 2.5$ in the initial stages of reaction. The simulations also require weak inhibition by TMSF,[25] a feature consistent with the pronounced line-broadening of the TMSF ^{19}F NMR signal that is observed as the siliconate speciation repopulates from $[(CF_3)_2SiMe_3]^-$ (K_1) to $[(CF_3)Si(F)Me_3]^-$ (K_5, where $K_1/K_5 \approx 8$)[19] during the final stages of consumption of **1** (see SI section 8.4).

Furthermore, equation 3 indicates that both the rate and selectivity of conversion of **1** to the C-H silylation product are proportional to the concentration ratio [RH]$_t$ / [**1**]$_t$. However, reducing the total concentration of **1**, limits the overall achievable conversion of the substrate (RH**)**. This limiting effect can be bypassed through slow-addition of **1** to the reaction. This maximizes [RH] / [**1**] and thus the productive fractionation, *f*, throughout the process, Scheme 4.

CONCLUSIONS

Using variable-ratio stopped-flow ^{19}F and ^{29}Si NMR spectroscopy, isotopic labelling, and DFT-calculations, the dual role of $TMSCF_3$ as a silylating reagent and source of base in the general process **1** + RH → RTMS + CF_3H, has been elucidated, Scheme 3. by using a series of 1,3-difluorobenzene substrates (**2**). As with reactions (i) and (ii), Scheme 1B, the vast majority of the active anion is present in siliconate reservoirs, primarily $[(CF_3)_2SiMe_3]^-$.[16,17,19]

The kinetics (equations 3, 5), KIE (k_H/k_D = 9.5) and LFER (ρ = + 5.5), indicate that irreversible deprotonation of RH (k_2) by the rapidly and reversibly liberated CF_3-anionoid is the rate-limiting step in the productive process yielding the C-H silylation product. Competing fluoride transfer[17] (k_3) from the CF_3-anionoid to $TMSCF_3$ (**1**) leads to a partition (k_2/k_3) that dictates the impact of the concentrations ([**1**] and [RH]) on the productive fractionation, *f*, equation 4. The fluoride transfer (k_3) generates TMSF and CF_2, which undergoes anion-catalyzed homologation (n) with **1** to generate further TMSF and perfluoroalkenes. This is detrimental not just to the efficiency of the C-H silylation with respect to **1**, but also causes inhibition, and eventual termination of catalysis (equations 3 and 5, $x \rightarrow 0$) by anion sequestration in $[C_{11}F_{23}]^-$ (**4**)[17,24] and analogous species.

Addition of an alkene (styrene **5**, Figure 5) to trap nascent CF_2, and slow addition of **1**, raise the productive fractionation, *f* (equation 4), attenuate homologation (n) and retard inhibition, Scheme 4. The TBAT initiates anionic catalysis, but other than controlling the rate (equations 3 and 5) its initial concentration does not affect the selectivity. Replacing $TMSCF_3$ (**1**) by the commercially-available, but more expensive reagent $TESCF_3$ (**7**) provides higher efficiency as a result of its lower reactivity (both K_1 and k_3) towards the CF_3-anionoid. By using a mixture of **1** and **7**, anion catalyzed CF_3 / F exchange (Scheme 2) allows

the bulkier reagent **7** to act as a surrogate source of CF_3 for TMS transfer, Figure 4B.

Overall, the CF_3-anionoid partitioning, *f*, is identified as the key parameter for both the lifetime of the active catalyst system, and the efficiency by which the silylating reagent is converted into the desired product. This conclusion leads to the general guidelines shown below for reactions involving anion-catalyzed silylation of a weak C-H acid (RH) by **1**.

- The anion pre-catalyst concentration does not influence the productive fractionation, but does affect the rate. When extensive anion-inhibition is evident (via ^{19}F NMR detection of $[C_{11}F_{23}]^-$, **4**) higher homogeneous catalyst loadings (e.g. TBAT in THF) can be employed. Kondo's conditions,[13] employing a heterogenous initiator (CsF in DME at 0 °) are highly effective, and the initiator can be used in excess.
- Addition of a sacrificial alkene to consume CF_2, strongly suppresses inhibition of the anion catalyst. High concentrations of alkene afford better selectivity, and thus use of a volatile electron-rich alkene (e.g. cyclohexene) in large excess will allow easy separation from the final reaction mixture, together with the difluorocyclopropanation product.
- Use of the minimum stoichiometry of silylating agent (**1**) required to effect full conversion of R-H to R-Si increases the rate and the efficiency. Slow, or aliquot-based addition of the silylating agent maintains a high ratio of [R-H]/[**1**], leading to greater productive fractionation.
- Use of a sterically bulky silyating agent, e.g. $TESCF_3$ (**7**) increases the dynamic concentration of the CF_3 anionoid, and reduces the extent of CF_2-generation, leading to higher rates and higher productive fractionation.

The results presented above may also aid in the design of reagents and conditions to expand the scope for generation and interception of transient carbanions by C-H deprotonation (k_2). Moreover, the readily-determined partitioning factor ($k_2/n.k_3$, Figure 3; $n \approx 2.5$ in THF at 300 K) may be useful in a more general sense to assess the relative kinetic acidity of other C-H species,[26] by monitoring the relative rates of evolution of CF_3H versus TMSF by ^{19}F NMR spectroscopy.[27]

AUTHOR INFORMATION

Corresponding Author

* guy.lloyd-jones@ed.ac.uk

Present Addresses

† G.T.T: Department of Chemistry, University of Victoria, PO Box 1700 STN CSC, Victoria, BC V8W 2Y2, Canada.
§ A. R. S. Departament de Química Analítica i Química Orgànica, Universitat Rovira i Virgili, C/ Marcel·lí Domingo 1, 43007 Tarragona, Catalonia.

Author Contributions

The manuscript was written through contributions of all authors.

Funding Sources

A.G.D. thanks the SNSF for a postdoctoral fellowship (P2ZHP2_181497). P.H.H.O. thanks the EC for an Erasmus+ grant. G.T.T. thanks Mitacs for a Globalink Research Award. A. R. S. thanks the EC for an Erasmus+ grant, AGUAR for a MOBINT-MIF 2020 grant, and the Santander Erasmus fund. The research leading to these results has received funding from the European Research Council under the European Union's Seventh Framework Programme (FP7/2007-2013) / ERC grant agreements n° [340163] and [838616].

Notes

The authors declare no competing financial interest.

ASSOCIATED CONTENT

Experimental details, reaction profiles and characterization data can be found in the Supporting Information. This material is available free of charge via the Internet at http://pubs.acs.org.

ACKNOWLEDGMENT

We thank Dr Andrew Leach (University of Manchester, UK) for valuable discussions on the mechanism and energetics of the reactive intermediates discussed herein, Professor Scott McIndoe (University of Victoria, Canada) for facilitating the collaborative research visit by G. T. T., Prof. Franziska Schoenebeck (Aachen) for facilitating the collaborative research visit by P. H. H. O., and Prof Elena Fernández (Tarragona) for facilitating the collaborative research visit by A. R. S. We thank the University of Edinburgh Compute and Data Facility (ECDF) for computing resources.

REFERENCES

(1) For selected reviews on $TMSCF_3$ in preparation of organofluorine molecules, see: (a) Liu, X.; Xu, C.; Wang, M.; Liu, Q. Trifluoromethyltrimethylsilane: Nucleophilic Trifluoromethylation and Beyond. *Chem. Rev.* **2015**, *115*, 683–730. (b) Zhu, W.; Wang, J.; Wang, S.; Gu, Z.; Aceña, J. L.; Izawa, K.; Liu, H.; Soloshonok, V. A. Recent Advances in the Trifluoromethylation Methodology and New CF_3-Containing Drugs. *J. Fluor. Chem.* **2014**, *167*, 37–54. (c) Prakash, G. K. S.; Yudin, A. K. Perfluoroalkylation with Organosilicon Reagents. *Chem. Rev.* **1997**, *97*, 757–786.

(2) For selected examples of the application of $TMSCF_3$ in anion catalyzed processes other than those in Scheme 1B, see: (a) Xie, Q.; Zhu, Z.; Li, L.; Ni, C.; Hu, J. Controllable Double CF_2-Insertion into sp^2 C-Cu Bond Using $TMSCF_3$: A Facile Access to Tetrafluoroethylene-Bridged Structures. *Chem. Sci.* **2020**, *11* , 276–280. (b) Wang, Q.; Ni, C.; Hu, M.; Xie, Q.; Liu, Q.; Pan, S.; Hu, J. From C1 to C3: Copper-Catalyzed Gem-Bis(Trifluoromethyl)Olefination of α-Diazo Esters with $TMSCF_3$. *Angew. Chem., Int. Ed.* **2020**, *59*, 8507–8511. (c) Nozawa-Kumada, K.; Osawa, S.; Ojima, T.; Noguchi, K.; Shigeno, M.; Kondo, Y. Transition-Metal-Free Trifluoromethylation of Benzyl Bromides Using Trifluoromethyltrimethylsilane and CsF in 1,2-Dimethoxyethane. *Asian J. Org. Chem.* **2020**, *9*, 765–768. (d) Smedley, C. J; Zheng, Q.; Gao, B.; Li, S.; Molino, A.; Duivenvoorden, H. M.; Parker, B. S.; Wilson, D. J. D.; Sharpless, K. B.; Moses, J. E. Bifluoride Ion Mediated SuFEx Trifluoromethylation of Sulfonyl Fluorides and Iminosulfur Oxydifluorides. *Angew, Chem. Int. Ed.* **2019**, *58*, 4552–4556. (e) Xie, Q.; Li, L.; Zhu, Z.; Zhang, R.; Ni, C.; Hu, J. From C1 to C2: $TMSCF_3$ as a Precursor for Pentafluoroethylation. *Angew. Chem, Int. Ed.* **2018**, *57*, 13211–13215. (f) Li, L.; Ni, C.; Xie, Q.; Hu, M.; Wang, F.; Hu, J. $TMSCF_3$ as a Convenient Source of CF_2=CF_2 for Pentafluoroethylation, (Aryloxy)Tetrafluoroethylation, and Tetrafluoroethylation. *Angew. Chem., Int. Ed.* **2017**, *56*, 9971−9975. (g) Krishnamoorthy, S.; Kothandaraman, J.; Saldana, J.; Prakash, G. K. S. Direct Difluoromethylenation of Carbonyl Compounds by Using $TMSCF_3$: The Right Conditions. *Eur. J. Org. Chem.* **2016**, 4965–4969. (h) Hashimoto, R.; Iida, T.; Aikawa, K.; Ito, S.; Mikami, K. Direct α-Siladifluoromethylation of Lithium Enolates

with Ruppert-Prakash Reagent via C-F Bond Activation. *Chem. Eur. J.* **2014**, *20*, 2750–2754

(3) For selected examples of oxidative transformations generating CF_3-radical, see: (a) Yang, X.; Tsui, G. C. Trifluoromethylation of Unactivated Alkenes with Me_3SiCF_3 and N-Iodosuccinimide. *Org. Lett.* **2019**, *21*, 1521–1525. (b) Yu, W.; Xu, X. H.; Qing, F. L. Silver-Mediated Oxidative Fluorotrifluoromethylation of Unactivated Alkenes. *Adv. Synth. Catal.* **2015**, *357*, 2039–2044. (c) Li, L.; Deng, M.; Zheng, S. C.; Xiong, Y. P.; Tan, B.; Liu, X. Y. Metal-Free Direct Intramolecular Carbotrifluoromethylation of Alkenes to Functionalized Trifluoromethyl Azaheterocycles. *Org. Lett.* **2014**, *16*, 504–507. (d) Wu, X.; Chu, L.; Qing, F.-L. Silver-Catalyzed Hydrotrifluoromethylation of Unactivated Alkenes with CF_3SiMe_3 . *Angew. Chem., Int. Ed.* **2013***, 52,* 2198 –2202. (e) Ye, Y.; Lee, S. H.; Sanford, M. S. Silver-Mediated Trifluoromethylation of Arenes Using $TMSCF_3$. *Org. Lett.* **2011**, *13*, 5464–5467.

(4) a) Ruppert, I.; Schlich, K.; Volbach, W.; Die Ersten CF_3-substituierten organyl(chlor)silane. *Tetrahedron Lett.* **1984**, *25*, 2195−2198. (b) Kruse, A.; Siegemund, G.; Schumann, A.; Ruppert, I. A process for the production of perfluoroalkyl compounds, and the pentafluoroethyl-trimethylsilane. German Pat. DE3805534, **1989**.

(5) (a) Prakash, G. K. S.; Krishnamurti, R.; Olah, G. A. Fluoride-Induced Trifluoromethylation of Carbonyl Compounds with Trifluoromethyltrimethylsilane (TMS-CF_3). A Trifluoromethide Equivalent. *J. Am. Chem. Soc.* **1989**, *111*, 393–395. (b) Ramaiah, P.; Krishnamurti, R.; Prakash, G. K. S. 1-Trifluoromethyl-1-cyclohexanol. *Org. Synth.* **1995**, *72*, 232−236. (c) Prakash, G. K. S.; Jog, P. V.; Batamack, P. T. D.; Olah, G. A. Taming of Fluoroform: Direct Nucleophilic Trifluoromethylation of Si, B, S, and C Centers. *Science* **2012**, *338*, 1324−1327.

(6) For recent reviews, see: (a) Dilman, A. D. Nucleophilic Di- and Trifluoromethylation of C=O and C=N Bonds. In *Modern Synthesis Processes and Reactivity of Fluorinated Compounds. Progress in Fluorince. Science Series.* Groult, H.; Leroux, F. R.; Tressaud, A., Eds; Elsevier. **2017**, pp 181–199. (b) Beier, P.; Zibinsky, M.; Prakash, S. G. K. Nucleophilic Additions of Perfluoroalkyl Groups. *Organic Reactions* **2016**, *91*, 1−492 and references therein.

(7) (a) Wang, F.; Luo, T.; Hu,J.; Wang, Y.; Krishnan, H. S.; Jog, P. V.; Ganesh, S. K.; Prakash, G. K. S.; Olah, G. A. Synthesis of gem-Difluorinated Cyclopropanes and Cyclopropenes; Trifluoromethyltrimethylsilane as a Difluorocarbene Source. *Angew. Chem., Int. Ed.* **2011**, *50*, 7153 –7157. (b) Hryshchuk, O. V.; Varenyk, A. O.; Yurov, Y.; Kuchkovska, Y. O.; Tymtsunik, A. V.; Grygorenko, O. O. Gem-Difluorocyclopropanation of Alkenyl Trifluoroborates with the CF_3SiMe_3–NaI System. *Eur. J. Org. Chem.* **2020***,* 2217–2224. (c) Nosik, P. S.; Poturai, A. S.; Pashko, M. O.; Melnykov, K. P.; Ryabukhin, S. V.; Volochnyuk, D. M.; Grygorenko, O. O. N-Difluorocyclopropyl-Substituted Pyrazoles: Synthesis and Reactivity. *Eur. J. Org. Chem.* **2019**, 4311–4319. (d) Nosik, P. S.; Ryabukhin, S. V.; Grygorenko, O. O.; Volochnyuk, D. M. Transition Metal-Free Gem-Difluorocyclopropanation of Alkenes with CF_3SiMe_3−NaI System: A Recipe for Electron-Deficient Substrates. *Adv. Synth. Catal.* **2018**, *360*, 4104–4114. (e) Bychek, R. M.; Levterov, V. V.; Sadkova, I. V.; Tolmachev, A. A.; Mykhailiuk, P. K. Synthesis of Functionalized Difluorocyclopropanes: Unique Building Blocks for Drug Discovery. *Chem Eur. J.* **2018**, *24*, 12291–12297, and references therein.

(8) (a) Panne, P.; Naumann, D.; Hoge, B. Cyanide Initiated Perfluoroorganylations with Perfluoroorgano Silicon Compounds. *J. Fluor. Chem.* **2001**, *112*, 283–286. (b) Adams, D. J.; Clark, J. H.; Hansen, L. B.; Sanders, V. C.; Tavener, S. J. Reaction of Tetramethylammonium Fluoride with Trifluoromethyltrimethylsilane. *J. Fluorine Chem*. **1998**, *92*, 123−125.

(9) Behr, J. B.; Chavaria, D.; Plantier-Royon, R. Trifluoromethide as a Strong Base: [CF_3^-] Mediates Dichloromethylation of Nitrones by Proton Abstraction from the Solvent. *J. Org. Chem.* **2013**, *78*, 11477–11482.

(10) Nishimine, T.; Taira, H.; Tokunaga, E.; Shiro, M.; Shibata, N. Enantioselective Trichloromethylation of MBH-Fluorides with Chloroform Based on Silicon-Assisted C-F Activation and Carbanion Exchange Induced by a Ruppert-Prakash Reagent. *Angew. Chem., Int. Ed.* **2016**, *55*, 359–363.

(11) (a) Ji, X.; Zhao, X.; Shi, H.; Cao, S. HMPA-Promoted Siladifluoromethylation of Di-, and Triarylmethanes with the Ruppert–Prakash Reagent. *Chem. Asian J.* **2017**, *12*, 2794–2798. (b) Fordyce, E. A. F.; Wang, Y.; Luebbers, T.; Lam, H. W. Copper-Catalyzed Silylation of Cyclopropenes Using (Trifluoromethyl) Trimethylsilane. *Chem. Commun.* **2008**, 1124–1126. (c) Adams, D. J.; Clark, J. H.; Hansen, L. B.; Sanders, V. C.; Tavener, S. J. Aromatic Trifluoromethyldenitration and Trifluoromethyldecyanation Using Trifluoromethyltrimethylsilane. *J. Chem. Soc., Perkin Trans. 1*, **1998**, 3081–3085.

(12) Takahashi, K.; Ano, Y.; Chatani, N. Fluoride Anion-Initiated Bis-Trifluoromethylation of Phenyl Aromatic Carboxylates with (Trifluoromethyl)Trimethylsilane. *Chem. Commun.* **2020**, *56*, 11661–11664. (b) Nozawa-Kumada, K.; Inagi, M.; Kondo, Y. Highly Chemoselective DMPU-Mediated Trialkylsilylation of Terminal Alkynes Using Trifluoromethyltrialkylsilane. *Asian J. Org. Chem.* **2017**, *6*, 63–66. (c) Arde, P.; Reddy, V.; Anand, R. V. NHC Catalysed Trimethylsilylation of Terminal Alkynes and Indoles with Ruppert's Reagent under Solvent Free Conditions. *RSC Adv.* **2014**, *4*, 49775–49779.; (d) Xiong, D. C.; Zhou, Y.; Cui, Y.; Ye, X. S. Synthesis of Triazolyl-Linked Polysialic Acids. *Tetrahedron* **2014**, *70*, 9405–9412. (e) Yoshimatsu, M.; Kuribayashi, M. A Novel Utilization of Trifluoromethanide as a Base: A Convenient Synthesis of Trimethylsilylacetylene. *J. Chem. Soc. Perkin Trans 1* **2001**, 1256–1257. (f) Ishizaki, M.; Hoshino, O. Unprecedented Cesium and Potassium Fluorides Catalyzed Trialkylsilylation and Tributylstannylation of Terminal Alkynes with Trifluoromethyl-Trialkylsilanes and -Tributylstannane. *Tetrahedron* **2000**, *56*, 8813–8819.

(13) (a) Nozawa-Kumada, K.; Osawa, S.; Sasaki, M.; Chataigner, I.; Shigeno, M.; Kondo, Y. Deprotonative Silylation of Aromatic C-H Bonds Mediated by a Combination of Trifluoromethyltrialkylsilane and Fluoride. *J. Org. Chem.* **2017**, *82*, 9487–9496.; (b) Sasaki, M.; Kondo, Y. Deprotonative C-H Silylation of Functionalized Arenes and Heteroarenes Using Trifluoromethyltrialkylsilane with Fluoride. *Org. Lett.* **2015**, *17*, 848–851.

(14) For an overview on arene C-H silylation strategies, see (a) Richter, S. C.; Oestreich, M. Emerging Strategies for C–H Silylation. *Trends Chem.* **2020**, *2*, 13–27.; (b) Fukumoto, Y., Chatani, N. Transition-Metal-Catalyzed C-H Bond Silylation. In *Organosilicon Chemistry. Novel Approaches and Reactions.* Hiyama, T.; Oestreich, M., Eds; Wiley-VCH. **2019**, pp 174–198.; (c) Transition-Metal-Free Catalytic C-H Bond Silylation. In *Organosilicon Chemistry. Novel Approaches and Reactions.* Hiyama, T.; Oestreich, M., Eds; Wiley-VCH. **2019**, pp 213–240.; (d) Zhou, B.; Lu, A.; Zhang, Y. Pd-Catalyzed C-H Silylation Reactions with Disilanes. *Synlett* **2019**, *30*, 685–693.; (e) Bähr, S.; Oestreich, M. Electrophilic Aromatic Substitution with Silicon Electrophiles: Catalytic Friedel–Crafts C−H Silylation. *Angew. Chem. Int. Ed.* **2017**, *56* (1), 52–59.

(15) For selected recent examples of applications of arylsilanes see: (a) Muraca, A. C. A.; Raminelli, C. Exploring Possible Surrogates for Kobayashi's Aryne Precursors. *ACS Omega* **2020**, *5*, 2440–2457.; (b) Luo, H.; Sun, K.; Xie, Q.; Li, X.; Zhang, X.; Luo, X. Copper-Mediated Phosphorylation of Arylsilanes with H-Phosphonate Diesters. *Asian J. Org. Chem.* **2020**, 2083–2086; (c) Dorel, R.; Boehm, P.; Schwinger, D. P.; Hartwig, J. F. Copper-Mediated Fluorination of Aryl Trisiloxanes with Nucleophilic Fluoride. *Chem. Eur. J.* **2020**, *26*, 1759–1762.; (d) Ball, L. T.; Corrie, T. J. A.; Cresswell A. J.; Lloyd-Jones, G. C. Kinetic Analysis of

Domino Catalysis: a Case Study on Gold-Catalyzed Arylation, *ACS Catal.,* **2020** *10,* 10420–10426.; (e) Minami, Y.; Hiyama, T. Designing Cross-Coupling Reactions Using Aryl(Trialkyl)Silanes. *Chem. Eur. J.* **2019**, *25* (2), 391–399.; (f) Hiyama, T.; Minami,Y.; Mori, A. Transition-Metal-Catalyzed Cross-coupling of Organosilicon Compounds. In *Organosilicon Chemistry. Novel Approaches and Reactions.* Hiyama, T.; Oestreich, M., Eds; Wiley-VCH. **2019**, pp 271–332.; (g) Ramesh, R.; Reddy, D. S. Quest for Novel Chemical Entities through Incorporation of Silicon in Drug Scaffolds. *J. Med. Chem.* **2018**, *61*, 3779–3798.; (h) Rayment, E. J.; Mekareeya, A.; Summerhill, N.; Anderson, E. A. Mechanistic Study of Arylsilane Oxidation through ^{19}F NMR Spectroscopy. *J. Am. Chem. Soc.* **2017**, *139*, 6138–6145.; (i) Komiyama, T.; Minami, Y.; Hiyama, T. Recent Advances in Transition-Metal-Catalyzed Synthetic Transformations of Organosilicon Reagents. *ACS Catal.* **2017**, *7* , 631–651.; (j) Mesgar, M.; Daugulis, O. Silylaryl Halides Can Replace Triflates as Aryne Precursors. *Org. Lett.* **2016**, *18*, 3910–3913.; see also: (k) Somfai, P.; Seashore-Ludlow, B. Organosilicon Reagents: Vinyl-, Alkynyl-, and Arylsilanes. In *Comprehensive Organic Synthesis II (Second Edition).* Knochel, P., Ed; Elsevier. **2014**, *1*, pp 27–48.

(16) Johnston, C. P.; West, T. H.; Dooley, R. E.; Reid, M.; Jones, A. B.; King, E. J.; Leach, A. G.; Lloyd-Jones, G. C. Anion-Initiated Trifluoromethylation by $TMSCF_3$: Deconvolution of the Siliconate-Carbanion Dichotomy by Stopped-Flow NMR/IR. *J. Am. Chem. Soc.* **2018**, *140*, 11112–11124.

(17) García-Domínguez, A.; West, T. H.; Primozic, J. J.; Grant, K. M.; Johnston, C. P.; Cumming, G. G.; Leach, A. G.; Lloyd-Jones, G. C. Difluorocarbene Generation from $TMSCF_3$: Kinetics and Mechanism of NaI-Mediated and Si-Induced Anionic Chain Reactions. *J. Am. Chem. Soc.* **2020**, *142*, 14649–14663

(18) Pilcher, A. S.; DeShong, P. Utilization of Tetrabutylammonium Triphenyldifluorosilicate as a Fluoride Source for Silicon–Carbon Bond Cleavage. *J. Org. Chem.* **1996**, *61*, 6901–6905.

(19) (a) Maggiarosa, N.; Tyrra, W.; Naumann, D.; Kirij, N. V.; Yagupolskii, Y. L. $[Me_3Si(CF_3)F]^-$ and $[Me_3Si(CF_3)_2]^-$: Reactive Intermediates in Fluoride-Initiated Trifluoromethylation with Me_3SiCF_3 - An NMR Study. *Angew. Chem., Int. Ed.* **1999**, *38*, 2252–2253. (b) Kolomeitsev, A.; Bissky, G.; Lork, E.; Movchun, V.; Rusanov, E.; Kirsch, P.; Röschenthaler, G.-V. Different fluoride anion sources and (trifluoromethyl)trimethylsilane: molecular structure of tris(dimethylamino)sulfonium bis(trifluoromethyl)-trimethylsiliconate, the first isolated pentacoordinate silicon species with five Si-C bonds. *Chem. Commun.* **1999**, 1017–1018.

(20) (a) Prakash, G. K. S.; Wang, F.; Zhang, Z.; Haiges, R.; Rahm, M.; Christe, K. O.; Mathew, T.; Olah, G. A. Long-Lived Trifluoromethanide Anion: A Key Intermediate in Nucleophilic Trifluoromethylations. *Angew. Chem., Int. Ed.* **2014**, *53*, 11575−11578. (b) Santschi, N.; Gilmour, R. The (Not So) Ephemeral Trifluoromethanide Anion. *Angew. Chem., Int. Ed.* **2014**, *53*, 11414−11415. (c) Lishchynskyi, A.; Miloserdov, F. M.; Martin, E.; Benet-Buchholz, J.; Escudero-Adań,E.C.; Konovalov, A.I.; Grushin,V.V. The Trifluoromethyl Anion. *Angew. Chem., Int. Ed.* **2015**, *54*, 15289−15293. (d) Miloserdov, F. M.; Konovalov, A. I.; Martin, E.; Benet-Buchholz, J.; Escudero-Adań, E.C.; Lishchynskyi, A.; Grushin,V.V. The Trifluoromethyl Anion: Evidence for $[K(crypt\text{-}222)]^+CF_3^-$. *Helv. Chim. Acta* **2017**, *100*, No. e1700032. (e) Harlow, R. L.; Benet- Buchholz, J.; Miloserdov, F. M.; Konovalov, A. I.; Marshall, W. J.; Martin, E.; Benet-Bucholz, J.; Escudero-Adań, E.C.; Martin, E.; Lishchynskyi, A.; Grushin, V. V. On the Structure of $[K(crypt\text{-}222)]^+CF_3^-$. *Helv. Chim. Acta* **2018**, *101*, No. e1800015

(21) The reactions are very sensitive to adventitious moisture from the atmosphere and were thus conducted in NMR tubes sealed with a J Youngs valve. To avoid dangerous pressures (CF_3H, b.p. –82 °C) we determined the head-space volume and ensured to use reagent concentrations that limited the maximum overpressure to 2 atm at 100% conversion of **1** to CF_3H.

(22) Because of the open-venting of the system at the terminus of the flow arrangement, the specific design of stopped-flow NMR system employed (see SI) is less hazardous (in terms of limiting reagent concentrations / CF_3H gas-evolution and over-pressures) than conducting the reactions in sealed NMR tubes. This allowed slightly higher concentrations of **1**, **7** and **2** to be employed.

(23) The correlation with σ, rather than σ^-, is consistent with the development of an anion orthogonal to the π-system of the aromatic ring, and the meta-orientation of the modifying substituent to the site of deprotonation (X, Figure 2D)

(24) (a) Tyrra, W.; Kremlev,M. M.; Naumann, D.; Scherer, H.; Schmidt, H.; Hoge, B.; Pantenburg, I. Yagupolskii, Y L. How Trimethyl(trifluoromethyl)silane Reacts with Itself in the Presence of Naked Fluoride—A One-Pot Synthesis of Bis([15]crown-5)cesium 1,1,1,3,5,5,5-Heptafluoro-2,4-bis(trifluoromethyl)pentenide. *Chem. Eur. J.* **2005***, 11*, 6514–6518. see also: ESI-MS detection of **4** reported in (b) Weske, S.; Schoop, R.; Koszinowski, K. The Role of Ate Complexes in the Copper-Mediated Trifluoromethylation of Alkynes. *Chem. Eur. J.* **2016**, *22*, 11310 – 11316.

(25) In principle, the Ph_3SiF and Ph_3SiCF_3 liberated through initiation by TBAT can also cause inhibition by siliconate generation. However, there was not any significant line-broadening evident in these species in the ^{19}F NMR spectra, see SI, and the process was not required or successful kinetic simulation.

(26) For studies on the pK_a of CF_3H see: a) Symons, E. A.; Clermont, M. J. Hydrogen Isotope Exchange between Fluoroform (CF_3H) and Water. 1. Catalysis by Hydroxide Ion. *J. Am. Chem. Soc.* **1981**, *103*, 3127–3130.; (b) Butin, K. P.; Kashin, A. N.; Beletskaya, I. P.; German, L. S.; Polishchuk, V. R. Acidities of some Fluorine Substituted C-H Acids. *J. Organomet. Chem.* **1970**, *25*, 11–16.; (c) Andreades, S. Fluorocarbanions. Rates of Base-Catalyzed Hydrogen-Deuterium Exchange, Isotope Effects, and Acidity of Monohydrofluorocarbons. *J. Am. Chem. Soc.* **1964**, *86*, 2003–2010.

(27) This requires that the C-H acid be irreversibly deprotonated and then rapidly silylated, i.e. k_4[**1**][R^-] >> k_2[CF_3][RH]. Competition of a C-H acid with, e.g. **2a**, can be used to determine if this condition is valid.

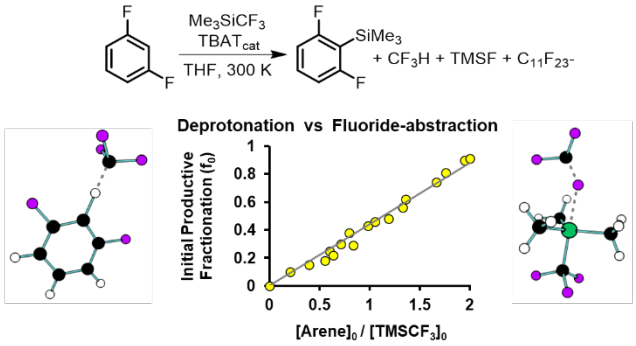

Table of Contents artwork